

# Long-distance entanglement and quantum communication in coupled cavity arrays

Salvatore M. Giampaolo<sup>1,2</sup> and Fabrizio Illuminati<sup>1,2,3,4</sup>

<sup>1</sup>*Dipartimento di Matematica e Informatica, Università degli Studi di Salerno,  
Via Ponte don Melillo, I-84084 Fisciano (SA), Italy*

<sup>2</sup>*CNR-INFM Coherentia, and INFN Sezione di Napoli,  
Gruppo collegato di Salerno, I-84084 Fisciano (SA), Italy*

<sup>3</sup>*ISI Foundation for Scientific Interchange, Viale Settimio Severo 65, 00173 Torino, Italy*

<sup>4</sup>*Corresponding author. Electronic address: illuminati@sa.infn.it*

(Dated: June 15, 2009)

We introduce quantum spin models that allow for long-distance end-to-end entanglement and long-distance, high-fidelity teleportation, even at moderately high temperatures. We show how these models, that realize an optimal compromise between scalability and resilience to decoherence, can be implemented in simply engineered arrays of coupled optical cavities. We demonstrate how the latter can be used to realize a quasi-deterministic scheme of long-distance quantum communication with high success rate, without direct projection on Bell states and Bell measurements.

PACS numbers: 03.65.Ca, 03.67.Mn, 73.43.Nq, 75.10.Jm

## INTRODUCTION

Experimental realizations of quantum communication [1] and information [2] protocols fall roughly in two different classes. The first one includes all-optical implementations, either with single photons [3, 4, 5], or with continuous variables [6]. In the optical setting, quantum communication is to a great extent decoherence-free and can be easily carried out over long distances. However, the scalability of all-optical devices is fundamentally limited, as the engineering of strong interactions between photons poses formidable challenges. The second class includes matter-based devices such as systems of trapped ions [7, 8], superconducting quantum dots [9], and NMR-based devices [10, 11]. Matter-based implementations, that in principle are easily scalable, suffer from hardly avoidable strong incoherent interactions with the environment. Moreover, single-site addressing is very difficult to realize in such systems. All schemes of quantum communication realized or proposed so far thus suffer from unsolved difficulties concerning either the distances covered, the control of decoherence, the extent of scalability, or yet the maximum fidelities achievable.

Recently, hybrid atom-optical systems of coupled cavity arrays (CCAs) have been intensively studied in relation to their ability to realize/simulate collective phenomena typical of strongly correlated systems [12, 13, 14, 15, 16]. In the present work we will show that CCAs also allow an optimal compromise between scalability and robustness against decoherence for quantum communication tasks. Namely, if properly engineered, they warrant an effective protection from unwanted environmental interactions, at least over the time scales typically needed for the processing of quantum information. Besides the extremely high controllability and the straightforward addressability of single constituents, CCAs also allow in

principle a great degree of flexibility in their design and geometry [17]. Therefore, they should be tested as natural candidates for the realization of spatially extended communication networks and scalable computation devices.

Regardless of the class in which they fall, typical schemes of quantum communication rely on properly engineered direct interactions. This requirement is a fundamental limitation, particularly so for realizations that suffer both from strong decoherence effects and limited mobility. From a general theoretical standpoint, an important step ahead has been obtained recently with the discovery that the ground state of a particular class of quantum spin models with a finite correlation length defined on one-dimensional chains with open ends can sustain “long-distance entanglement” (LDE), i.e. finite and large values of the entanglement between the end points, even for systems of very large size [18, 19, 20].

In this work we present a novel scheme for the realization of long-distance and high-fidelity quantum communication based on the phenomenon of LDE, and we demonstrate its experimental realizability in suitably engineered CCAs. We first introduce a class of spin models with open ends and suitably defined end-bond interactions. Next, we discuss how these “ $\lambda$ - $\mu$ ” models sustain end-to-end LDE and allow for schemes of long-distance and high-fidelity teleportation, even at moderately high temperature and in the presence of noise. We then demonstrate how these spin channels that couple scalability and resilience to decoherence can be implemented by properly engineered one-dimensional CCAs. Finally, by exploiting the high degree of control and flexibility of CCAs, we introduce quasi-deterministic schemes of teleportation with high success rates without direct projection on Bell states and Bell measurements, thus overcoming one of the major difficulties that typically

beset matter-based quantum communication devices.

### THE $\lambda$ - $\mu$ MODEL AND LDE

Consider quantum spin models on a one-dimensional lattice of length  $N$ , with open ends, and general site-dependent nearest-neighbor interactions of the  $XX$  type:

$$H_s = - \sum_{k=1}^{N-1} J_k (S_k^x S_{k+1}^x + S_k^y S_{k+1}^y), \quad (1)$$

where  $J_k$  is the set of the  $N - 1$  nearest-neighbor couplings and  $S_k^\alpha$  denotes the Spin-1/2 operators at site  $k$  ( $\alpha = x, y$ ). The pure  $XX$  limit is recovered when  $J_k = J, \forall k$ . The model is exactly solvable by Jordan-Wigner diagonalization, both for chains of finite size and in the thermodynamic limit [21]. For arbitrary site-dependent couplings, the associated models are still exactly solvable by a straightforward extension of the techniques developed in Ref. [21], albeit, in general, only numerically [20, 22, 23]. For these models, the phenomenon of perfect ground-state LDE (maximal end-to-end concurrence independent of the size of the chain) sets on when the Hamiltonian  $H_s$  is dimerized, with perfectly alternated weak and strong couplings:  $J_k \equiv J_{odd}$  ( $k = 1, 3, \dots, N - 1$ ),  $J_k \equiv J_{even}$  ( $k = 2, 4, \dots, N - 2$ ), and  $J_{odd} \ll J_{even}$  [20]. Normalizing all couplings by  $J_{even}$ , and renaming the rescaled odd coupling:  $J_{odd}/J_{even} \equiv \lambda$ , the condition for perfect LDE reads  $\lambda \ll 1$  [20]. Ground-state quasi-perfect LDE (maximal end-to-end concurrence slowly decaying with the size of the chain) is realized by models with uniform bulk (b) interactions and weak end bonds (eb):  $J_2 = J_3 = \dots = J_{N-2} \equiv J_b$ ,  $J_1 = J_{N-1} \equiv J_{eb}$ . Rescaling all couplings by  $J_b$  (with  $J_{eb}/J_b \equiv \lambda$ ), the condition for quasi-perfect LDE reads  $\lambda \ll 1$  [20]. In the first instance (*dimerized  $XX$  model*) the energy gap closes exponentially with the size of the system, making this system useless for realistic applications at finite temperature. In the second instance (the  $\lambda$  *model*) the gap closes with an algebraic power law, but useful amounts of LDE can survive only at extremely low temperatures, unreachable at present and in the immediately foreseeable future [20]. Here we introduce a  $\lambda$ - $\mu$  *model* that realizes an optimal compromise between the requirements of strong LDE in a system of large size, robustness of LDE at moderately high temperatures, and ease of realistic implementations. The  $\lambda$ - $\mu$  model is defined by Hamiltonian (1) with uniform bulk interactions and alternating weak end bonds (eb) and strong near-end bond (neb) interactions:  $J_3 = J_4 = \dots = J_{N-3} \equiv J_b$ ,  $J_2 = J_{N-2} \equiv J_{neb}$ , and  $J_1 = J_{N-1} \equiv J_{eb}$ . Normalizing all interactions by  $J_b$ , and redefining the scaled couplings  $J_{eb}/J_b \equiv \lambda$  and  $J_{neb}/J_b \equiv \mu$ , the condition for an optimized end-to-end LDE is  $\lambda \ll 1 \ll \mu$ .

The LDE properties of the  $\lambda$ - $\mu$  chain, at zero and finite

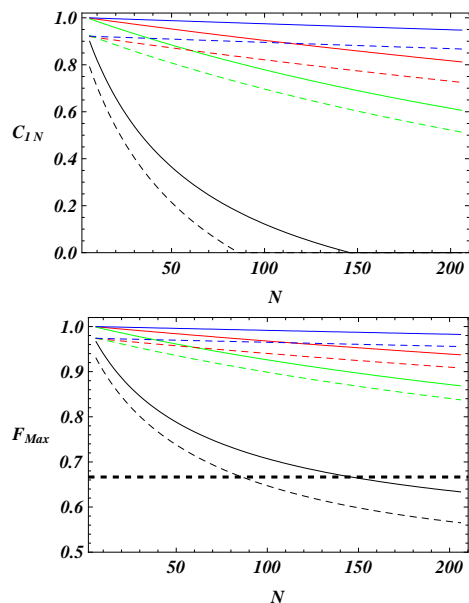


FIG. 1: Upper panel: Concurrence  $C_{1N}$  between the end points of a  $\lambda$ - $\mu$  spin chain as a function its length  $N$ , for different values of the end bonds  $\lambda$  and  $\mu$ , at zero (solid lines) and at finite temperature (dashed lines). Solid blue line:  $\lambda = 0.15$ ,  $\mu = 7.0$ . Solid red line:  $\lambda = 0.2$ ,  $\mu = 5.0$ . Solid green line:  $\lambda = 0.4$ ,  $\mu = 3.0$ . Solid black line, for comparison:  $C_{1N}$  of a  $\lambda$  spin chain (i.e. with  $\mu = 1$ ) for  $\lambda = 0.2$ . Dashed lines:  $C_{1N}$  as a function of  $N$  at different reduced temperatures  $T/J_b$  for the same sets of values of  $\lambda$  and  $\mu$  as above. Dashed blue line:  $T/J_b = 0.0005$ . Dashed red line:  $T/J_b = 0.0001$ . Dashed green line:  $T/J_b = 0.001$ . Dashed black line, for comparison:  $C_{1N}$  of the corresponding  $\lambda$  spin chain at a temperature  $T/J_b = 0.0006$ . Lower Panel: The maximal fidelity of teleportation  $\mathcal{F}_{max}$  between the end points of the  $\lambda$ - $\mu$  spin chain as a function of  $N$ , at zero and finite temperature, for the same sets of values reported in the upper panel. In the case of the  $\lambda$  model (black lines),  $\mathcal{F}_{max}$  sinks below the classical threshold  $2/3$  (horizontal dashed line), for the corresponding vanishing values of the end-to-end concurrence (See upper panel).

temperature, are reported in the upper panel of Fig. 1, where the end-to-end concurrence is plotted as a function of the size of the chain. In the lower panel of Fig. 1 we report the behavior of the corresponding maximal fidelity of teleportation  $\mathcal{F}_{max}$ , which, in the case of non-vanishing spin-spin concurrence, is a monotonic function of the pairwise end-to-end entanglement [20, 24]. Fig. 1 shows that interacting spin systems of the  $\lambda$ - $\mu$  type conjugate efficiently resilience to decoherence and scalability, as further confirmed by comparing with the performance of systems of the  $\lambda$  type.

### THE $\lambda$ - $\mu$ CHANNEL BY CCAS

Consider a linear CCA with open ends, consisting of  $N$  cavities. The dynamics of a single constituent of the

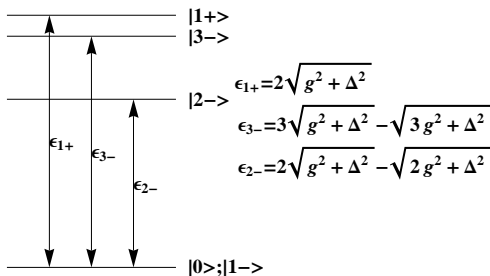


FIG. 2: Representation of the energy levels for a cavity with  $\omega = \sqrt{g^2 + \Delta^2}$ . The ground state is two-fold degenerate, and the energy gap  $\varepsilon_{2-}$  prevents the occupancy of the higher energy levels, thus realizing an effective two-level system.

array doped with a single two-level atom is well described by the Jaynes-Cummings Hamiltonian

$$H_k = \omega a_k^\dagger a_k + \omega' |e_k\rangle \langle e_k| + g a_k^\dagger |g_k\rangle \langle e_k| + g |e_k\rangle \langle a_k| a_k, \quad (2)$$

where  $a_k$  ( $a_k^\dagger$ ) is the annihilation (creation) operator of photons with energy  $\omega$  in the  $k$ -th cavity,  $|g_k\rangle$  and  $|e_k\rangle$  are respectively the ground and excited atomic states, separated by the gap  $\omega'$ , and  $g$  is the photon-atom coupling strength. The local Hamiltonian Eq. (2) is immediately diagonalized in the basis of dressed photonic and atomic excitations (polaritons):

$$\begin{aligned} |\emptyset_k\rangle &= |g_k\rangle |0_k\rangle; \\ |n+\rangle_k &= \cos \theta_n |g_k\rangle |n_k\rangle + \sin \theta_n |e_k\rangle |(n-1)_k\rangle \quad n \geq 1; \\ |n-\rangle_k &= \sin \theta_n |g_k\rangle |n_k\rangle - \cos \theta_n |e_k\rangle |(n-1)_k\rangle \quad n \geq 1, \end{aligned} \quad (3)$$

where  $\theta_n$  is given by  $\tan 2\theta_n = -g\sqrt{n}/\Delta$  and  $\Delta = \omega' - \omega$  is the atom-light detuning. Each polariton is characterized by an energy equal to

$$\varepsilon_0 = 0; \quad \varepsilon_{n\pm} = n\omega \pm \sqrt{ng^2 + \Delta^2}. \quad (4)$$

When  $\omega = \sqrt{g^2 + \Delta^2}$  the ground state of Eq. (2) becomes two-fold degenerate, resulting in a superposition of  $|\emptyset_k\rangle$  and  $|1-\rangle_k$ , see Fig. 2. If both the atom-cavity interaction energy and the working temperature are small compared to  $\varepsilon_{2-} = 2\sqrt{g^2 + \Delta^2} - \sqrt{2g^2 + \Delta^2}$ , one may neglect all the local polaritonic states but  $|\emptyset_k\rangle$  and  $|1-\rangle_k$ . This situation defines a local two-level system. Adjacent cavities can be easily coupled either by photon hopping or via wave guides of different dielectric and conducting properties. The wave function overlap of two adjacent cavities introduces the associated tunneling elements, so that the total Hamiltonian of the CCA reads:

$$H_{cca} = \sum_k^N H_k - \sum_k^{N-1} J_k (a_k^\dagger a_{k+1} + a_{k+1}^\dagger a_k). \quad (5)$$

Each hopping amplitude  $J_k$  depends strongly on both the geometry of the cavities and the actual overlap between adjacent cavities. If the maximum value among all the

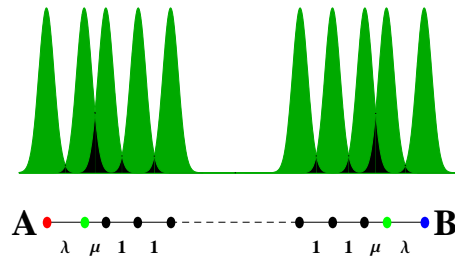


FIG. 3: Scheme of a CCA realizing a  $\lambda$ - $\mu$  linear spin chain. Dark green: Area covered by the wave functions associated to each site of the array. The two next-to-end sites (light green circles) are symmetrically displaced closer to their neighbors in the bulk (black circles) and thus the overlap (black area) between the wave functions of these two cavities and their neighbors in the bulk is larger than the would-be reference (unit) overlap in an equispaced CCA. At the same time, the overlap between the end sites of the array (red and blue circles) and the next-to-end sites is reduced proportionally compared to the equispaced array.

couplings  $\{J_k\}$  is much below the energy of the first excited state:  $\max\{J_k\} \ll \varepsilon_{2-}$ , then the total Hamiltonian Eq. (5) can be mapped in a spin-1/2 model of the  $XX$  type with site-dependent couplings of the form Eq. (1), where the state  $|\emptyset_k\rangle$  ( $|1-\rangle_k$ ) plays the role of  $|\downarrow_k\rangle$  ( $|\uparrow_k\rangle$ ). The mapping to an open-end  $\lambda$ - $\mu$  linear spin chain is then realized, e.g., by simply tuning the distance between the end- and next-to-end sites of the CCA, as showed in Fig. 3. The  $\lambda$ - $\mu$  chain is thus realized starting from an equispaced CCA with site-independent nearest-neighbor bulk coupling amplitude  $J_b$ , and then moving the second and the  $N-1$ -th cavities from their original position towards the bulk. This shift lowers below unity the reduced coupling between the end points of the array and their next-to-end neighbors ( $J_1/J_b = J_{N-1}/J_b = \lambda < 1$ ), and increases above unity the reduced coupling between the next-to-end sites and their neighbors in the bulk ( $J_2/J_b = J_{N-2}/J_b = \mu > 1$ ).

### LONG-DISTANCE AND HIGH-FIDELITY QUANTUM COMMUNICATION IN $\lambda$ - $\mu$ CCAS

We now demonstrate that CCAs in the  $\lambda$ - $\mu$  configuration allow for long-distance and high-fidelity quantum communication in fully realistic conditions at moderately high temperatures. In Fig. 4 we report the fidelity of teleportation  $F_{max}$  as a function of the reduced couplings  $\lambda$  and  $\mu$  for different temperatures. Remarkably, Fig. 4 shows the existence of a rather high *critical* temperature of teleportation for CCAs in the  $\lambda$ - $\mu$  configuration. The region of the physical parameters compatible with a nonclassical fidelity  $F_{max} > 2/3$  is progressively reduced with increasing temperature, until it disappears at  $T_c \approx 0.13J_b$ . Similar behaviors are observed for longer

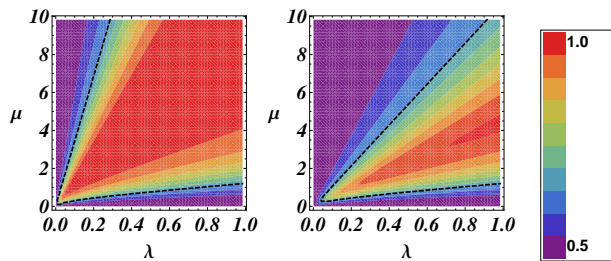


FIG. 4: Fidelity of teleportation  $F_{max}$  in a  $\lambda$ - $\mu$  configuration, determined by exact numerical diagonalization, for a CCA of  $N = 12$  cavities as a function of the reduced couplings  $\lambda = J_1/J_b$  and  $\mu = J_2/J_b$  at different reduced temperatures  $T/J_b$ . Left panel:  $T/J_b = 0.005$ . Right panel:  $T/J_b = 0.01$ .  $F_{max}$  varies between 0.5 (violet) and 1 (red). The dashed black line denotes the classical threshold  $F_{max}^c = 2/3$ .

CCAs, with  $T_c$  slowly decreasing with the length of the array. For instance, for an array of  $N = 36$  cavities in the  $\lambda$ - $\mu$  configuration, the critical temperature of transition to *bona fide* quantum teleportation is  $T_c \approx 0.11J_b$ .

A formidable obstacle to the concrete realization of working quantum teleportation devices is performing the projection over a Bell state, in order for the sender to teleport a quantum state faithfully to the receiver. In fact, in the framework of condensed matter there hardly exist quantities, easily available in current and foreseeable experiments, that admit as eigenstates any two-qubit Bell states. In the following, we will demonstrate a simple and concrete scheme for long-distance, high-fidelity quantum communication and teleportation in  $\lambda$ - $\mu$  CCAs that realizes naturally some recent theoretical proposals to realize Bell-state projections indirectly, by matching together free evolutions and local measurements of easily controllable experimental quantities [25, 26, 27]. We first illustrate it in the simplest case of an array of only two cavities at zero temperature, with the first cavity accessible by the sender and the second one by the receiver. The sender has access also to another cavity, the "0" cavity, that stores the state to be teleported  $|\varphi\rangle = \alpha|\uparrow_0\rangle + \beta|\downarrow_0\rangle$ . The entire system is initially in the state:

$$|\Psi(0)\rangle = \frac{1}{\sqrt{2}}(\alpha|\uparrow_0\rangle + \beta|\downarrow_0\rangle)(|\uparrow_1\rangle|\downarrow_2\rangle + |\downarrow_1\rangle|\uparrow_2\rangle). \quad (6)$$

If  $J_0 \gg J_1$ , under time evolution one has:

$$|\Psi(t)\rangle = \frac{1}{\sqrt{2}}[\alpha|\uparrow_0\rangle|\uparrow_1\rangle|\downarrow_2\rangle + \beta|\downarrow_0\rangle|\downarrow_1\rangle|\uparrow_2\rangle \\ + |\uparrow_0\rangle|\downarrow_1\rangle(\alpha\cos(J_0t)|\uparrow_2\rangle - i\beta\sin(J_0t)|\downarrow_2\rangle) \\ + |\downarrow_0\rangle|\uparrow_1\rangle(-i\alpha\sin(J_0t)|\uparrow_2\rangle + \beta\cos(J_0t)|\downarrow_2\rangle)]. \quad (7)$$

If at time  $t = \pi/(4J_0)$  the sender measures the local magnetizations ( $S_0^z$ ,  $S_1^z$ ) in the first two cavities, He/She will obtain with probability 1/2 that the state sent to the receiver is the image of  $|\varphi\rangle$  under the action of a local rotation. The value 1/2 for the probability stems

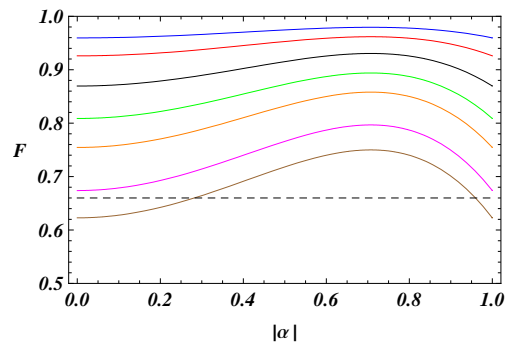


FIG. 5: Fidelity of teleportation through a  $\lambda$ - $\mu$  CCA channel of  $N = 12$  cavities, for a generic input state  $|\varphi\rangle = \alpha|\uparrow_0\rangle + \beta|\downarrow_0\rangle$ , as a function of  $|\alpha|$  for different temperatures. Blue line:  $T = 0.005J_b$ ; Red line:  $T = 0.0075J_b$ ; Black line:  $T = 0.01J_b$ ; Green line:  $T = 0.0125J_b$ ; Orange line:  $T = 0.015J_b$ ; Magenta line:  $T = 0.02J_b$ ; Brown line:  $T = 0.025J_b$ . We have set  $\lambda = 0.8$ ,  $\mu = 4.1$ , and  $\nu = 50$ . The horizontal dashed line denotes the classical threshold  $F_{max}^c = 2/3$ .

from the fact that any simultaneous eigenstate of  $S_0^z$  and  $S_1^z$  can be obtained with equal probability but one may discard the case in which the total magnetization is equal to  $\pm 1$ . Realizing a local rotation of  $\pm\pi/2$  around  $S_2^z$ , with the sign depending on the result of the measurement that the sender communicates classically to the receiver, the latter recovers the original state  $|\varphi\rangle$  with unit fidelity.

The simple protocol described above can be immediately extended to  $\lambda$ - $\mu$  CCAs of any size, at finite temperature, and without imposing the constraint  $J_1 \ll J_0$ . By resorting again to exact diagonalization, in Fig. 5 we report the behavior of the fidelity of teleportation, as a function of  $|\alpha|$  of the state  $|\varphi\rangle$ , in the case of an array of  $N = 12$  cavities, with  $\nu \equiv J_0/J_b = 50$  and for different temperatures. Also in the non-ideal case the communication protocol has probability 1/2 of success. The fidelity depends on the input state, with a maximum for inputs with  $|\alpha| = |\beta|$  and a minimum for inputs with  $|\alpha| = 0, 1$ . The fidelity remains above 0.95 for all values of  $|\alpha|$  at moderately low temperatures.

In conclusion, we have demonstrated the feasibility of long-distance, high-fidelity quantum communication channels employing suitably engineered CCAs that simulate  $\lambda$ - $\mu$  open spin chains. The latter are characterized by an end-to-end entanglement that is much more resilient to decoherence compared to other spin systems supporting long-distance entanglement, like the  $XX$  open chain with dimerized interactions or models with uniform bulk interactions and weakly interacting end probes. Thus the  $\lambda$ - $\mu$  model, efficiently realized through simple configurations of open-end CCAs, provides a good quantum channel that can be exploited for faithful long-distance quantum communication. In the crucial case of quantum teleportation we have illustrated that, exploiting basic properties of optical cavities, it is possible to design a

simple and efficient quasi-deterministic protocol that allows a high rate of success without Bell measurements.

### ACKNOWLEDGEMENTS

We acknowledge financial support from the EC under the FP7 STREP Project HIP, from MIUR under the FARB fund, from INFN, from CNR-INFN Research and Development Center "Coherentia", and from ISI Foundation.

- 
- [1] C. H. Bennett, G. Brassard, C. Crépeau, R. Jozsa, A. Peres, and W. K. Wootters, *Phys. Rev. Lett.* **70**, 1895 (1993).
- [2] M. A. Nielsen and I. L. Chuang, *Quantum Computation and Quantum Information* (Cambridge University Press, Cambridge, 2000).
- [3] D. Bouwmeester, J.-W. Pan, K. Mattle, M. Eibl, H. Weinfurter, and A. Zeilinger, *Nature* **390**, 575 (1997).
- [4] D. Boschi, S. Branca, F. De Martini, L. Hardy, and S. Popescu, *Phys. Rev. Lett.* **80**, 1121 (1998);
- [5] R. Ursin *et al.*, *Nature* **430**, 849 (2004).
- [6] H. Yonezawa, T. Aoki, and A. Furusawa, *Nature* **431**, 430 (2004).
- [7] M. Riebe *et al.*, *Nature* **429**, 734 (2004).
- [8] M. D. Barrett *et al.*, *Nature* **429**, 737 (2004).
- [9] D. Fattal, E. Diamanti, K. Inoue, and Y. Yamamoto, *Phys. Rev. Lett.* **92**, 037904 (2004).
- [10] M. A. Nielsen, E. Knill, and R. Laflamme, *Nature* **395**, (1998).
- [11] G. Brassard, S. L. Braunstein, and R. Cleve, *Physica D* **120**, 43 (1998).
- [12] M. J. Hartmann, F. G. S. L. Brandão, and M. B. Plenio, *Nature Phys.* **2**, 849 (2006).
- [13] A. D. Greentree, C. Tahan, J. H. Cole, and L. C. L. Hollenberg, *Nature Phys.* **2**, 856 (2006).
- [14] D. G. Angelakis, M. F. Santos, and S. Bose, *Phys. Rev. A* **76**, 031805(R) (2007).
- [15] D. Rossini and R. Fazio, *Phys. Rev. Lett.* **99**, 186401 (2007).
- [16] M. J. Hartmann, F. G. S. L. Brandão, and M. B. Plenio, *Phys. Rev. Lett.* **99**, 160501 (2007).
- [17] M. J. Hartmann, F. G. S. L. Brandão, and M. B. Plenio, *Laser & Photon. Rev.* **2**, 527 (2008).
- [18] L. Campos Venuti, C. Degli Esposti Boschi, and M. Roncaglia, *Phys. Rev. Lett.* **96**, 247206 (2006).
- [19] L. Campos Venuti, C. Degli Esposti Boschi, and M. Roncaglia, *Phys. Rev. Lett.* **99**, 060401 (2007).
- [20] L. Campos Venuti, S. M. Giampaolo, F. Illuminati, and P. Zanardi, *Phys. Rev. A* **76**, 052328 (2007).
- [21] E. Lieb, T. Schultz, and D. Mattis, *Ann. Phys. (N.Y.)* **16**, 407 (1961).
- [22] S. M. Giampaolo and F. Illuminati, unpublished.
- [23] A. Wojcik *et al.*, *Phys. Rev. A* **72**, 034303 (2005).
- [24] M. Horodecki, P. Horodecki, and R. Horodecki, *Phys. Rev. A* **60**, 1888 (1999).
- [25] S.-B. Zheng, *Phys. Rev. A* **69**, 064302 (2004).
- [26] L. Ye and G.-C. Guo, *Phys. Rev. A* **70**, 054303 (2004).
- [27] W. B. Cardoso, A. T. Avelar, B. Baseia, and N. G. de Almeida, *Phys. Rev. A* **72**, 045802 (2005).